



Supporting Information

for *Adv. Funct. Mater.*, DOI: 10.1002/adfm.202009382

Supramolecular Peptide Nanofibrils with Optimized Sequences and Molecular Structures for Efficient Retroviral Transduction

*Stefanie Sieste, Thomas Mack, Edina Lump, Manuel Hayn, Desiree Schütz, Annika Röcker, Christoph Meier, Kübra Kaygisiz, Frank Kirchhoff, Tuomas P. J. Knowles, Francesco S. Ruggeri, * Christopher V. Synatschke, * Jan Münch, * and Tanja Weil**

Supplementary Information for
Supramolecular Peptide Nanofibrils with Optimized Sequences and
Molecular Structures for Efficient Retroviral Transduction

*Stefanie Sieste, Thomas Mack, Edina Lump, Manuel Hayn, Desiree Schütz, Annika Röcker,
Christoph Meier, Kübra Kaygisiz, Frank Kirchhoff, Tuomas P. J. Knowles, Francesco S.
Ruggeri,* Christopher V. Synatschke,* Jan Münch,* and Tanja Weil**

S. Sieste, T. Mack, K. Kaygisiz, Dr. C. V. Synatschke, Prof. T. Weil
Department Synthesis of Macromolecules
Max Planck Institute for Polymer Research
Ackermannweg 10, 55128 Mainz, Germany
Email: weil@mpip-mainz.mpg.de, synatschke@mpip-mainz.mpg.de

S. Sieste, T. Mack, Dr. C. Meier, Prof. T. Weil
Institute of Inorganic Chemistry I
Ulm University
Albert-Einstein-Allee 11, 89081 Ulm, Germany

Dr. E. Lump, M. Hayn, D. Schütz, Dr. A. Röcker, Prof. F. Kirchhoff, Prof. J. Münch
Institute of Molecular Virology
Ulm University Medical Center
Meyerhofstraße 1, 89081 Ulm, Germany
Email: jan.muench@uni-ulm.de

Prof. T. P. J. Knowles, Prof. F. S. Ruggeri
Department of Chemistry
University of Cambridge
Cambridge CB2 1EW, UK
Email: fsr26@cam.ac.uk

Prof. T. P. J. Knowles
Cavendish Laboratory
University of Cambridge
Cambridge CB3 0HE, UK

Prof. F. S. Ruggeri

Laboratory of Physical Chemistry, Stippeneng 4, 6703 WE, Wageningen University, the Netherlands
Email: simone.ruggeri@wur.nl

Prof. J. Münch

Core Facility of Functional Peptidomics
Ulm University Medical Center
Albert-Einstein-Allee 47, 89081 Ulm, Germany

Methods

Materials for peptide synthesis and characterization

PyBOP, HBTU, Fmoc-Lys(Boc)-OH, Fmoc-Phe-OH, Fmoc-Gln(Trt)-OH, Fmoc-Ile-OH, Fmoc-Cys(Trt)-OH, Fmoc-Trp(Boc)-OH, Fmoc-Asn(Trt)-OH, Fmoc-Met-OH, Fmoc-Glu(OtBu)-OH, Fmoc-Ala-OH, Fmoc-Phe-Wang resin, Fmoc-Ile-Wang resin, Fmoc-Gln(Trt)-Wang resin and Fmoc-Met-Wang resin were purchased from Novabiochem®. N-ethyldiisopropylamine for synthesis (DIPEA) and potassium chloride (KCl) were obtained from Merck. Piperidine (\geq 99.5% for peptide synthesis) and trifluoroacetic acid (TFA, \geq 99.9%) were obtained from Carl Roth. Dimethylformamide (DMF, peptide synthesis), diethyl ether and acetonitrile (HiPerSolv Chromanorm for HPLC-gradient grade) were purchased from VWR Chemicals Prolabo. Dimethylsulfoxid (DMSO, ACS reagent, \geq 99.9%) was purchased from Honeywell, Riedel-de Haën®. Vivaspin 500 tubes (3 kDa MWCO) were purchased from Sartorius. Syringe filters Chromafil®Xtra RC-20/13 (0.20 μm) were obtained from Machery-Nagel. Uranyl acetate was purchased from Merck. Fluorescamine was purchased from PanReac AppliChem. PBS and α -Cyano-4-hydroxycinnamic acid were purchased from Sigma Aldrich. Proteostat® was purchased from Enzo Life Sciences. All chemicals were used as received unless explicitly stated otherwise. Some PNF sequences were purchased from Phtd Peptides industrial Co. limited with purity of \geq 95% (marked with ** in Supporting Table S3).

1. Synthesis of PNF derivatives

The peptides were synthesised according to standard Fmoc solid phase peptide synthesis on a microwave assisted peptide synthesizer (Liberty I by CEM or a Biotage Initiator+) in a 0.1 mmol scale. The C- to N-terminal coupling was achieved by using Wang resins preloaded with the first Fmoc-protected amino acid. Fmoc-deprotections were carried out with DMF solutions containing 20% or 25% v/v piperidine. Coupling reactions with 5 equiv. Fmoc-protected amino acid solutions in DMF at 75 °C for 5 or 10 min were catalysed by addition of 5 equiv. HBTU or PyBOP and 10 equiv. DIEA. Cleavage of the resin and final deprotection of the side chains were performed with a mixture of TFA, TIS and H₂O at a ratio of 95:2.5:2.5 by shaking at RT for 2h. The cleaved peptides were precipitated in cold diethyl ether and lyophilized. The final products were analysed with mass spectrometry measured on a Bruker Reflex III matrix assisted laser desorption/ionization time of flight (MALDI-TOF) MS device. 4-Hydroxy- α -cyanocinnaminic acid served as matrix.

2. Purification of PNF derivatives

All peptides were purified via HPLC using an optimized binary gradient (0.1% TFA water-acetonitrile as mobile phase). For preparative scale a Shimadzu system was used (LC-20AP, CBM-20A, SPD-20A) with a reversed phase C18 column (LiChrospher, Merck). Purity was verified by MALDI-TOF-MS (Bruker Reflex III) and analytical HPLC using a 1260 Infinity Quarternary LC System (Agilent Technologies) with an analytical ChroCART® 125-4

column (LiChrospher, Merck). All data can be found in Figure S12 and Table S3 (Supporting Information).

3. Preparation of PNF fibrils

The peptides were dissolved in DMSO ($c = 10$ mg/mL, stored at 4°C before usage) and added dropwise to PBS buffer to a final incubation concentration of 650 μ M or 1 mg/mL as indicated in the text. Other concentrations described in the text were achieved by further dilution of preformed PNFs.

4. TEM characterization of PNFs

5 μ L of pre-assembled PNF fibrils (1 mg/mL) were placed on copper grids which were coated with a thin electron-transparent Formvar-layer and freshly etched with oxygen plasma before use. After 5 min incubation time, the grids were washed three times with ddH₂O (double-distilled water) followed by sample staining with 2% uranyl acetate solution for 5 min. After additional three washing steps excess solvent was removed by filter paper. Measurements were performed on a Jeol 1400 electron microscope with 100 kV acceleration voltage or with an EM 109 transmission electron microscope (Zeiss) at an acceleration voltage of 80 kV.

5. ATR FT-IR

For ATR FT-IR spectroscopy measurements, 50 μ L of the respective 1 mg/mL PNF solution was lyophilized and the resulting powder used for measurement. All spectra were recorded on a Bruker Tensor 27 spectrometer with a diamond crystal as ATR element (PIKE MiracleTM,

spectral resolution 4 cm^{-1}). Every sample was measured with 20 scans. Data were analyzed with OriginPro (OriginLab) software.

6. Zeta potential

50 μL of preformed PNF fibrils (1 mg mL^{-1}) were diluted to 1 mL in an aqueous solution of 1 mM KCl. The dilution ratio was adjusted, if the count rate was not sufficient. The zeta potential was derived from the electrophoretic mobility of the peptides and measured using a Zeta Nanosizer ZS (Malvern Instruments) with 1 mL disposable folded capillary cells (Zetasizer Nano series, Malvern). Each measurement was performed in triplicates.

7. Laser scanning microscopy

For cell-binding studies 60 000 TZM-bl cells were seeded in 8-well IBIDI slides and stained the following day with Hoechst for 5 min at 37°C . 180 μL preformed PNF fibrils were stained with 20 μL diluted Proteostat Amyloid plaque detection kit solution according to suppliers' protocols (Enzo Life Science) to get a final concentration of 5 $\mu\text{g/ml}$. After 5 min, fibril mixtures were transferred to TZM-bl cells. The interaction of fibril clusters with cells was monitored after 30 min incubation time on a Leica confocal microscope with laser excitation wavelengths of 405 nm (Hoechst) and 561 nm (Proteostat). After 1h incubation, samples were washed three times with PBS and analysed again. For MLV-binding studies 180 μl preformed and Proteostat stained fibrils were mixed with 20 μl MLV-YFP and incubated for 10 min. to get a final concentration of 50 $\mu\text{g/ml}$. Then the mixture was added to an 8-well IBIDI slide and analysed after sedimentation with laser excitation of 488 nm (YFP) and 561 nm (Proteostat).

8. Conversion rate

For the determination of the amount of peptide monomer converting into fibrils, we established a fluorescence-based assay using amine reactive dye fluorescamine.^[1] Each PNF was incubated in PBS for 1 d with a concentration of 1 mg/mL (200 µL). 100 µL sample was centrifuged using a Vivaspin 500 tube (3kDa MWCO) to separate free monomers from fibrils (16.06 g, 4°C, 45 min). The other 100 uL of the sample served as a reference (original sample). Both the filtrate and the original sample were lyophilized and then dissolved in 25 µL DMSO. In a black 384-well-plate (Greiner Bio-one) 10 µL of DMSO sample (original sample and filtrate) was added and mixed with 3 uL of fluorescamine solution (3 mg/mL, DMSO). Fluorescence enhancement was measured with an excitation wavelength of $\lambda_{ex}= 365$ nm and an emission wavelength of $\lambda_{em}= 470$ nm with multiple reads 3x3 (Infinite® M1000 PRO microplate reader) after 20 mins of incubation. All values were calculated as n-fold fluorescence enhancement (DMSO-only as a reference was set to 1). The conversion rate CR was defined according to the following equation:

$$CR = 100 - \frac{100 \times \text{Fluorescence Intensity (Filtrate)}}{\text{Fluorescence Intensity (Original)}} [\%]$$

9. Proteostat® assay

Fluorescence spectra were recorded on an Infinite® M1000 PRO microplate reader (Tecan). 9 µL of sample aliquots (incubated for 1d in PBS at 1 mg/mL) were placed in black UV Star® 384 microliter well-plates (Greiner bio-one). A ProteoStat® solution was prepared according to manufacturers' protocol and diluted hundred-fold in PBS. After addition of 1 µL of Proteostat® solution to every sample and 10 mins of incubation time, the fluorescence

emission was recorded at 603 nm upon excitation at 550 nm with multiple reads per well (3x3).

10. Effect of PNF on HIV-1 infection

HIV-1 NL4-3 (R5) virus stocks were generated by calcium phosphate transfection as described before.^[2] 10000 TZM-bl cells (a HeLa cell line derivative that expresses high amounts of human CD4, CCR5 and CXCR4 and contain a β-galactosidase gene under the control of the HIV-1 long terminal repeat (LTR) promotor) were seeded into 96-well plates in 100 µL DMEM. On the next day, 80 µL fresh medium was added to the cells. 40 µL dilutions of EF-C or PNF solutions were prepared in PBS and mixed 1:1 (v/v) with 40 µL virus (pre-diluted 1:30 (v/v) in cell culture medium) by resuspending. After 10 min incubation to allow binding of virus particles to fibrils, 20 µL of virus-fibril mixture was added to 180 µL of cells. 3 days post infection, viral infectivity was determined using a galactosidase screen kit from Tropix as recommended by the manufacturer. β-Galactosidase activities were quantified as relative light units (RLU) per second with an Orion Microplate luminometer (Berthold).

11. CellTiter-Glo assay

TZM-bl cells were seeded in 96 well plates (~6000 cells/well). On the following day, 50 µL of fibril samples (130 µM) were added and serial diluted to the final concentrations of 65, 13, 2.6 and 0 µM. 50 µL of CellTiter-Glo mix was added and shaken for 2 mins. After 10 mins

50 µL were transferred to white plates and luminescence was recorded using an Orion microplate luminometer (Berthold).

12. Generation of lenti- and γ-retroviral vectors

800 000 HEK293T cells were seeded in 2 ml DMEM one day prior to the transfection. Cells were cotransfected with 250 µl OptiMEM containing 2.5 µg DNA and 7.5µl TransIT-LT1. For GALV pseudotyped γ-retrovirus, plasmids were used in a ratio 3:1:2.5 (pcmE26-gfp : GALV : pCsGPPA-ed). For VSV-G pseudotyped pSEW LUC2, plasmids were used in a ratio 2:2:1 (pSEW-luc: VSV-G : delta8.9). 64 h after transfection, virus was harvested, centrifuged for 3 min at 1300 rpm and stored at -80°C. VSV-G pseudotyped HIV-1 NL4-3 Firefly-Luciferase reporter virus stocks were generated using the calcium phosphate transfection method. For this, env-deficient proviral NL4-3 plasmid DNA and VSV-G env plasmid DNA were inoculated with CaCl₂ and ultrapure water before being mixed with 1x HBS. After incubation for 10 min at room temperature, the 200 µL of the transfection mix were added to 650,000 HEK293T cells/well seeded one day prior to the transfection in 6W plates. 16 hours post transfection, transfection mix was removed from the cells and cell culture medium was replaced with fresh medium. 48 hours post transfection, virus stocks were harvested, characterized by p24 ELISA and frozen at -80°C. HIV-1 NL4-3 (R5) virus stocks were generated by calcium phosphate transfection as described before.^[3]

13. Effect of PNF on VSV-G pseudotyped lentiviral transduction

To determine the effect of PNF on VSV-G pseudotyped HIV-1 or VSV-G pseudotyped pSEW LUC2 transduction, 10 000 cells were seeded in 96W microtiter plates. The next day, virus stocks were inoculated for 10 minutes with either EF-C or PNF-13 to allow binding of virus particles to fibrils. Indicated fibril concentrations were achieved during this inoculation step.

180 µL cells were subsequently infected with 20 µL of these PNF/VS mixtures in triplicates to achieve the indicated final concentrations of p24/mL on the cells. Three days post infection, infection rates were determined using the Firefly luciferase reporter assay (Promega). Firefly-Luciferase activities were quantified as relative light units (RLU) per second with an Orion Microplate luminometer (Berthold).

14. Effect of PNF on GALV pseudotyped γ-retroviral transduction

PBMCs were isolated using lymphocyte separation medium (Biocoll separating solution; Biochrom, Berlin, Germany). CD4 +T cells were isolated using the RosetteSep Human CD4 +T Cell Enrichment Cocktail (Stem Cell Technologies, Vancouver, Canada). Primary cells were cultured in RPMI-1640 containing 10% fetal calf serum (FCS), 2 mM glutamine, streptomycin (100 µg ml⁻¹), penicillin (100 U ml⁻¹), and 66 IU ml⁻¹ = 10 ng ml⁻¹ interleukin 2 (IL-2). Before infection, primary cells were stimulated for three days with phytohemagglutinin (PHA) (1 µg ml⁻¹). 20 000 CD4 +T cells were seeded into 96-well plates in 100 µl RPMI. Next day, 80 µl fresh medium was added to the cells. Dilutions of EF-C or PNF-13 were prepared in 80µl volume and mixed with 80µl virus (virus was diluted 1:8 in RPMI without FCS). After 10 min incubation to allow binding of virus particles to fibrils, 20µl of virus-fibril mixture was added to 180 µl cells. 3 days post infection percentage of GFP+ cells were determined by flow cytometry.

Supporting Tables

Table S1. Qualitative fibril formation determined via transmission electron microscopy (“+” for fibrils, and “-” for no fibrils/aggregates). Ability to bind Proteostat (“Prot bind.”, “+” for ≥ 10 n-fold fluorescence enhancement and “-” for ≤ 10 n-fold fluorescence enhancement). Zeta potential calculated by electrophoretic mobility. Conversion rate (“CR”) as the percentage of monomers converting into a fibril. Entries marked with * have previously been published.^[1]

PNF name	sequence	TEM	Prot bind.	Zeta potential [mV]	CR [%]
PNF-1	CKIKQIINMWQ	+	+	+11.8 \pm 0.4	50
PNF-2	CKIKQIINM	+	+	+19.1 \pm 0.5	45*
PNF-3	CKIKQII	+	+	+0.6 \pm 1.5	55*
PNF-4	KIKQIINMWQ	+	+	+10.8 \pm 0.2	86
PNF-5	KIKQIINM	+	+	+16.5 \pm 0.5	43
PNF-6	KIKQII	-	-	-	6
PNF-7	CKIK <u>IQ</u> INMWQ	+	+	+10.7 \pm 2.8*	87*
PNF-8	CKIK <u>IQ</u> INM	+	+	+22.3 \pm 0.6*	72*
PNF-9	CKIK <u>IQI</u>	+	+	+17.4 \pm 1.1*	54*
PNF-10	KIK <u>IQ</u> INMWQ	+	+	+17.2 \pm 0.7	93*
PNF-11	KIK <u>IQ</u> INM	+	+	+41.9 \pm 1.1*	64*
PNF-12	KIK <u>IQI</u>	-	-	-	5*
PNF-13	CKAKAQANMWQ	+	-	-4.4 \pm 3.2	92
PNF-14	CKAKAQANM	+	-	-3.7 \pm 0.9	38
PNF-15	CKAKAQA	+	-	-9.1 \pm 1.6	44
PNF-16	CKFKFQFNMWQ	+	+	+14.1 \pm 0.8	96
PNF-17	CKFKFQFNM	+	-	+15.9 \pm 0.4	88
PNF-18	CKFKFQF	+	+	+22.3 \pm 1.4*	95*
PNF-19	CEIEIQINMWQ	+	+	-35.8 \pm 1.2	74
PNF-20	CEIEIQINM	+	+	-38.6 \pm 5.2	43
PNF-21	CEIEIQI	+	+	-41.9 \pm 1.1	59
PNF-S1	KAKAQANMWQ	+	+	-19.6 \pm 1.7	65
PNF-S2	KAKAQANM	+	n.d.	n.d.	n.d.
PNF-S3	KAKAQA	+	n.d.	n.d.	n.d.
PNF-S4	KFKFQFNMWQ	+	-	+27.4 \pm 0.3	94

PNF-S5	KFKFQFNM	+	-	+20.1 ± 1.9*	91
PNF-S6	KFKFQF	+	-	-	83*
PNF-S7	MKIKIQI	+	-	10.1 ± 0.9	51
PNF-S8	MKFQFNWQ	+	-	+8.8 ± 0.5	75
PNF-S9	CSISIQINM	+	+	-31.7 ± 2.8	86
PNF-S10	CSISIQI	+	+	-31.8 ± 1.5	82

Table S2. Average RLU/s in infectivity assays of the peptides over multiple experiments at 13 and 65 µM.

PNF name	sequence	Avg Infection [RLU s ⁻¹] (13-65 µM)
PNF-1	CKIKQIINMWQ	1.8E+5
PNF-7	CKIK <u>Q</u> IINMWQ	1.9E+5
PNF-16	CKFKFQFNWQ	2.2E+5
PNF name	sequence	Avg Infection [RLU s ⁻¹] (13-65 µM)
PNF-4	KIKQIINMWQ	0.9E+5
PNF-10	KIK <u>Q</u> IINMWQ	1.4E+5
PNF-S4	CKFKFQFNWQ	0.55E+5
PNF name	sequence	Avg Infection [RLU s ⁻¹] (13-65 µM)
PNF-3	CKIKQII	0.05E+5
PNF-9	CKIK <u>Q</u> I	1.55E+5
PNF-18	CKFKFQF	1.8E+5
PNF-S7	MKIKIQI	0.19E+5
PNF-S8	MKFQFNWQ	0.23E+5
PNF name	sequence	Avg Infection [RLU s ⁻¹] (13-65 µM)
PNF-2	CKIKQIINM	2.95E+5
PNF-8	CKIK <u>Q</u> IINM	2.1E+5
PNF-17	CKFKFQFNM	1.9E+5
PNF name	sequence	Avg Infection [RLU s ⁻¹] (13-65 µM)
PNF-5	KIKQIINM	0.95E+5
PNF-11	KIK <u>Q</u> IINM	0.9E+4
PNF-S5	KFKFQFNM	1.25E+5
PNF name	sequence	Avg Infection [RLU s ⁻¹] (13-65 µM)
PNF-6	KIKQII	0.04E+5
PNF-12	KIK <u>Q</u> I	0.1E+5
PNF-S6	KFKFQF	0.1E+5

Table S3. Collected fractions for all peptides after purification with HPLC, see Supplementary Fig. 12. Calculated mass and assignments for all signals found in mass spectra with an intensity of at least 10 % in relation to the main peak. Entries marked with * have previously been published.^[1] PNF marked with ** have been purchased from Phtd Peptides industrial Co. limited with purit \geq 95%.

SAP name	fraction collected [min]	calc. exact mass [g mol ⁻¹]	m/z found
PNF-1	10.90 to 11.89	1403.74	1404.75 [M+H] ⁺ , 1416.75 [unknown], 1420.75 [M+O+H] ⁺ , 2807.48 [2M-2H+H] ⁺ , 2823.48 [2M-2H+O+H] ⁺
PNF-2*	9.81 to 10.79	1089.60	976.57 [M-ASN+H] ⁺ , 1090.61 [M+H] ⁺ , 1112.59 [M+Na] ⁺ , 1196.65 [M+Anisyl+H] ⁺ , 2065.15 [unknown], 2179.20 [2M-2H+H] ⁺ , 2201.18 [2M-2H+Na] ⁺
PNF-3*	9.63 to 10.05	844.52	845.53 [M+H] ⁺ , 867.51 [M+Na] ⁺ , 1034.57 [M+CHCA+H] ⁺ , 1688.03 [2M-2H+H] ⁺ , 1710.01 [2M-2H+Na] ⁺
PNF-4	10.42 to 11.02	1300.73	1301.74 [M+H] ⁺
PNF-5	9.55 to 10.12	986.59	987.60 [M+H] ⁺ , 1003.60 [M+O+H] ⁺
PNF-6	9.09 to 9.65	741.51	742.52 [M+H] ⁺ , 764.50 [M+Na] ⁺
PNF-7*	10.29 to 11.28	1403.74	1404.75 [M+H] ⁺ , 1420.74 [M+O+H] ⁺ , 1426.73 [M+Na] ⁺ , 1436.74 [unknown], 1452.73 [unknown], 2807.47 [2M-2H+H] ⁺
PNF-8*	10.25 to 10.67	1089.60	976.57 [M-ASN+H] ⁺ , 1090.61 [M+H] ⁺ , 1003.60 [M+O+H] ⁺ , 2065.16 [unknown], 2179.20 [2M-2H+H] ⁺
PNF-9	9.96 to 10.48	844.52	845.53 [M+H] ⁺ , 857.53 [unknown], 867.51 [M+Na] ⁺ , 1688.03 [2M-2H+H] ⁺ , 1710.02 [2M-2H+Na] ⁺ , 1725.99 [unknown]
PNF-10*	10.65 to 11.29	1300.73	1301.74 [M+H] ⁺ , 1317.74 [M+O+H] ⁺ , 1323.55 [M+Na] ⁺ , 1349.73 [unknown]
PNF-11*	9.96 to 10.49	986.59	987.60 [M+H] ⁺ , 1003.60 [M+O+H] ⁺

PNF-12*	9.82 to 10.29	741.51	742.52 [M+H] ⁺ , 764.50 [M+Na] ⁺
PNF-13	8.95 to 9.68	1277.60	1278.61 [M+H] ⁺
PNF-14**	n.d.	963.46	n.d.
PNF-15**	n.d.	718.38	n.d.
PNF-16	10.99 to 11.98	1505.69	1506.70 [M+H] ⁺ , 1522.70 [M+O+H] ⁺ , 1528.69 [M+Na] ⁺
PNF-17	10.84 to 11.48	1191.56	1192.56 [M+H] ⁺ , 1204.56 [unknown]
PNF-18*	10.78 to 11.38	946.47	947.48 [M+H] ⁺ , 1136.52 [M+CHCA+H] ⁺ , 1892.94 [2M-2H+H] ⁺
PNF-19**	n.d.	1405.64	n.d.
PNF-20**	n.d.	1091.50	n.d.
PNF-21**	n.d.	846.42	n.d.
PNF-S1	8.16 to 9.15	1174.59	1175.60 [M+H] ⁺ , 1191.60 [M+O+H] ⁺ , 1223.59 [unknown]
PNF-S2**	n.d.	860.45	n.d.
PNF-S3**	n.d.	615.37	n.d.
PNF-S4	11.16 to 11.80	1402.69	1403.69 [M+H] ⁺ , 1419.69 [M+O+H] ⁺ , 1435.69 [unknown], 1451.68 [unknown]
PNF-S5*	10.09 to 11.08	1088.55	1089.55 [M+H] ⁺ , 1105.55 [M+O+H] ⁺ , 1111.54 [M+Na] ⁺
PNF-S6*	10.64 to 11.41	843.46	844.47 [M+H] ⁺ , 866.45 [M+Na] ⁺
PNF-S7	10.25 to 10.79	872.55	873.56 [M+H] ⁺ , 889.55 [M+O+H] ⁺ , 895.54 [M+Na] ⁺ , 911.52 [M+K] ⁺
PNF-S8	9.99 to 10.98	974.50	975.51 [M+H] ⁺ , 991.51 [M+O+H] ⁺
PNF-S9**	n.d.	1007.48	n.d.
PNF-S10**	n.d.	762.39	n.d.

Supporting Figures

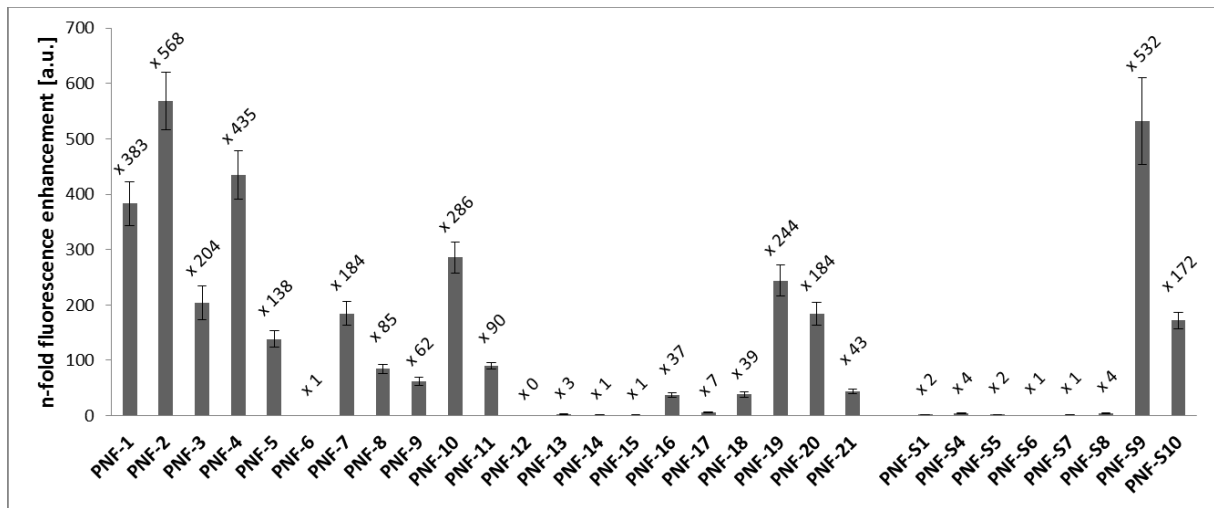


Figure S1: Proteostat® assay showing n-fold fluorescence enhancement of preformed PNF samples at 1 mg mL⁻¹.

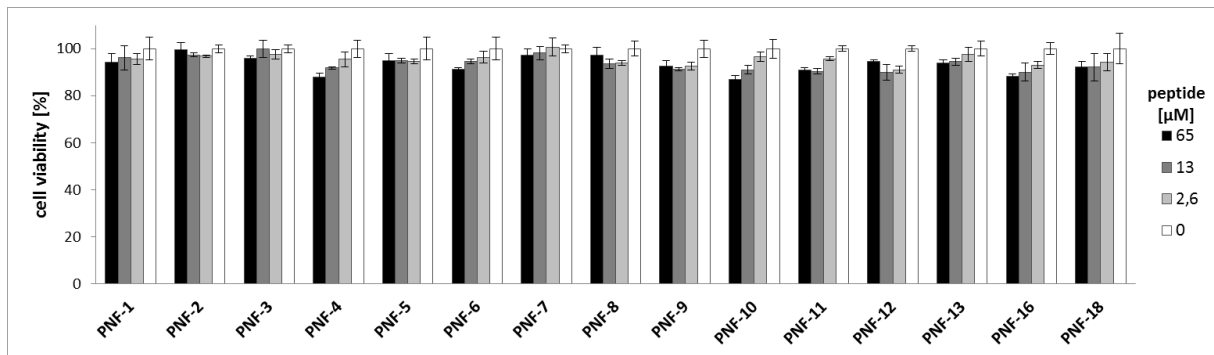


Figure S2: CellTiter-Glo cell viability assay of TZM-bl cells treated with increasing concentrations of PNFs. Values shown indicate mean values derived from biological triplicate ± standard deviation.

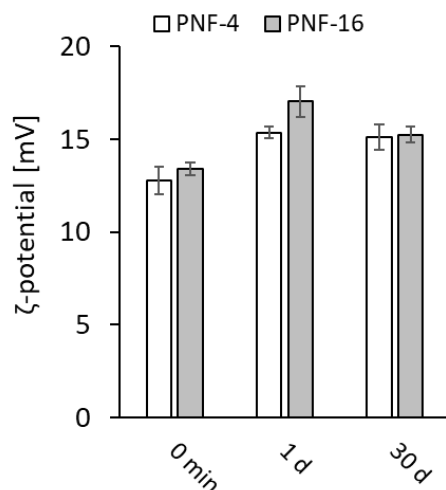


Figure S3: Time-dependent ζ -potential measurements of PNF-4 and PNF-16.

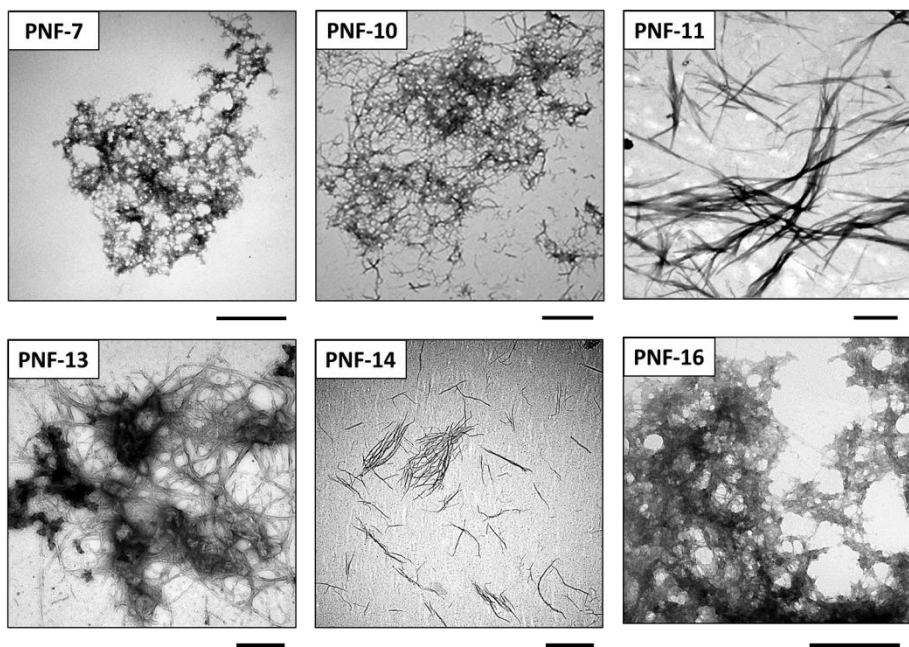


Figure S4: Representative TEM micrographs of PNF assemblies. Scale bars represent 500 nm.

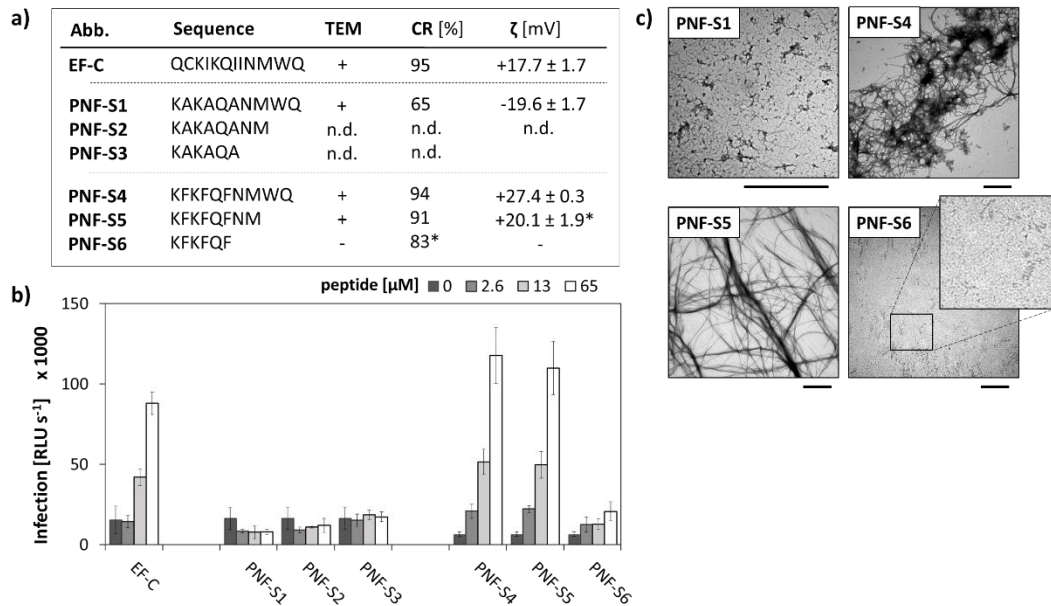


Figure S5: a) Tabular list of alanine and phenylalanine containing peptide derivatives, including the ability to form PNFs for PNF-S1, PNF-S4 and PNF-S5 as observed in TEM measurements with + = fibrils and - = no aggregate formation detected. Monomer-to-fibril conversion rates (CR) were determined in a fluorescence-based assay. High values indicate a large percentage of peptides participating in fibril formation. Zeta potential values for PNF solutions. b) Transduction enhancement assay showing HIV-1 infection rates of TZM-bl cells observed in the presence of increasing concentrations of PNF. Shown are mean values derived from triplicate infections ± standard deviation. RLU/s; relative light units per second. c) Representative TEM micrographs of PNF assemblies. Scale bars represent 500 nm. Entries marked with * have previously been published.^[1]

a)

Abb.	Sequence	TEM	CR [%]	ζ [mV]
PNF-9	CKIKIQI	+	54*	+17.4 ± 1.1
PNF-S7	MKIKIQI	+	51	+10.1 ± 0.9
PNF-18	CKFKFQF	+	95*	+22.3 ± 1.4
PNF-S8	MKFQFQF	+	75*	+8.8 ± 0.5

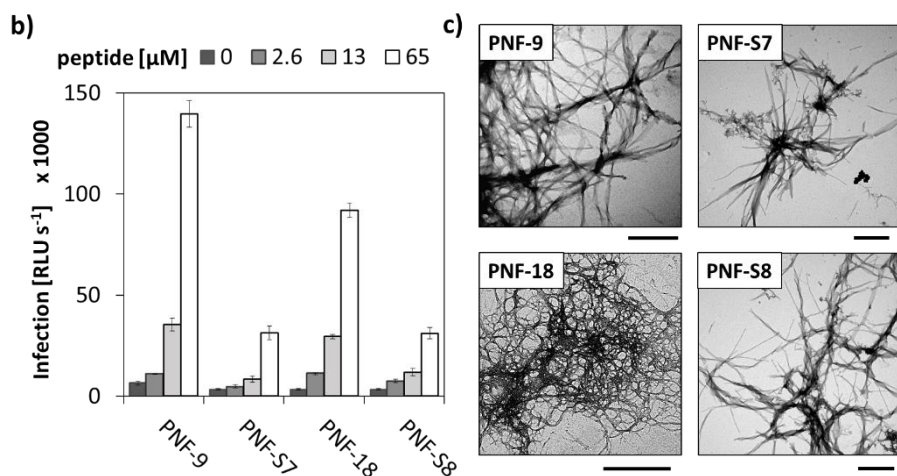


Figure S6: a) Tabular list of cysteine and methionine containing peptide derivatives, including the ability to form PNFs as observed in TEM measurements with + = fibrils and - = no aggregate formation detected. Monomer-to-fibril conversion rates (CR) were determined in a fluorescence-based assay. High values indicate a large percentage of peptides participating in fibril formation. Zeta potential values for PNF solutions. b) Transduction enhancement assay showing HIV-1 infection rates of TZM-bl cells observed in the presence of increasing concentrations of PNF. Shown are mean values derived from triplicate infections ± standard deviation. RLU/s; relative light units per second. c) Representative TEM micrographs of PNF assemblies. Scale bars represent 500 nm. Entries marked with * have previously been published.^[1]

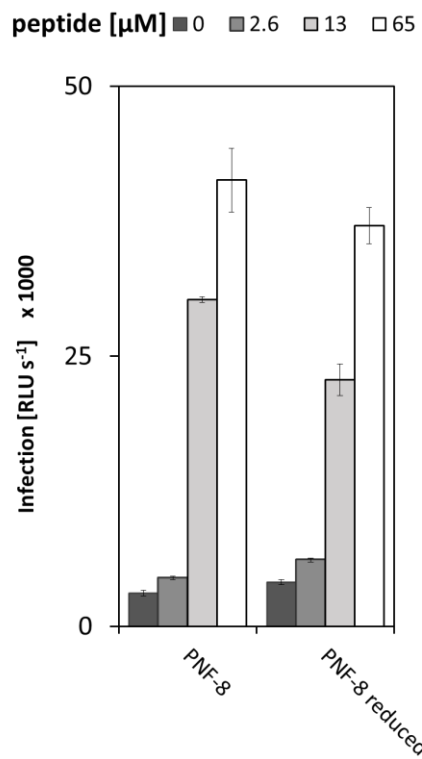


Figure S7: Transduction enhancement assay showing HIV-1 infection rates of TZM-bl cells observed in the presence of increasing concentrations of PNF. Shown are mean values derived from triplicate infections \pm standard deviation. RLU/s; relative light units per second. PNF-8 and PNF-8 treated with 1 eq TCEP before inducing self-assembly.

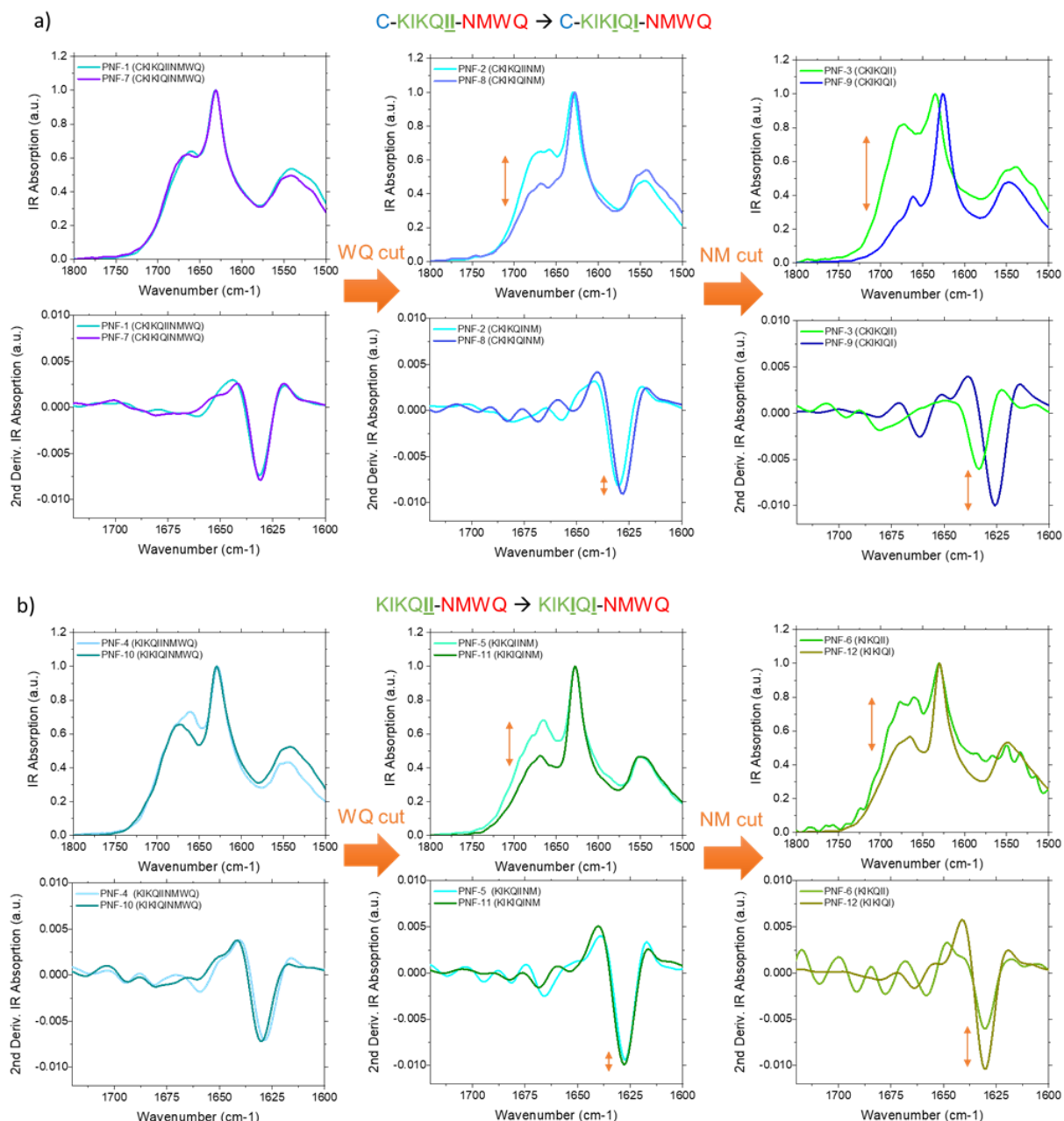


Figure S8: Structural variability upon intrinsic switch in a) presence and b) absence of the N-terminal cysteine.

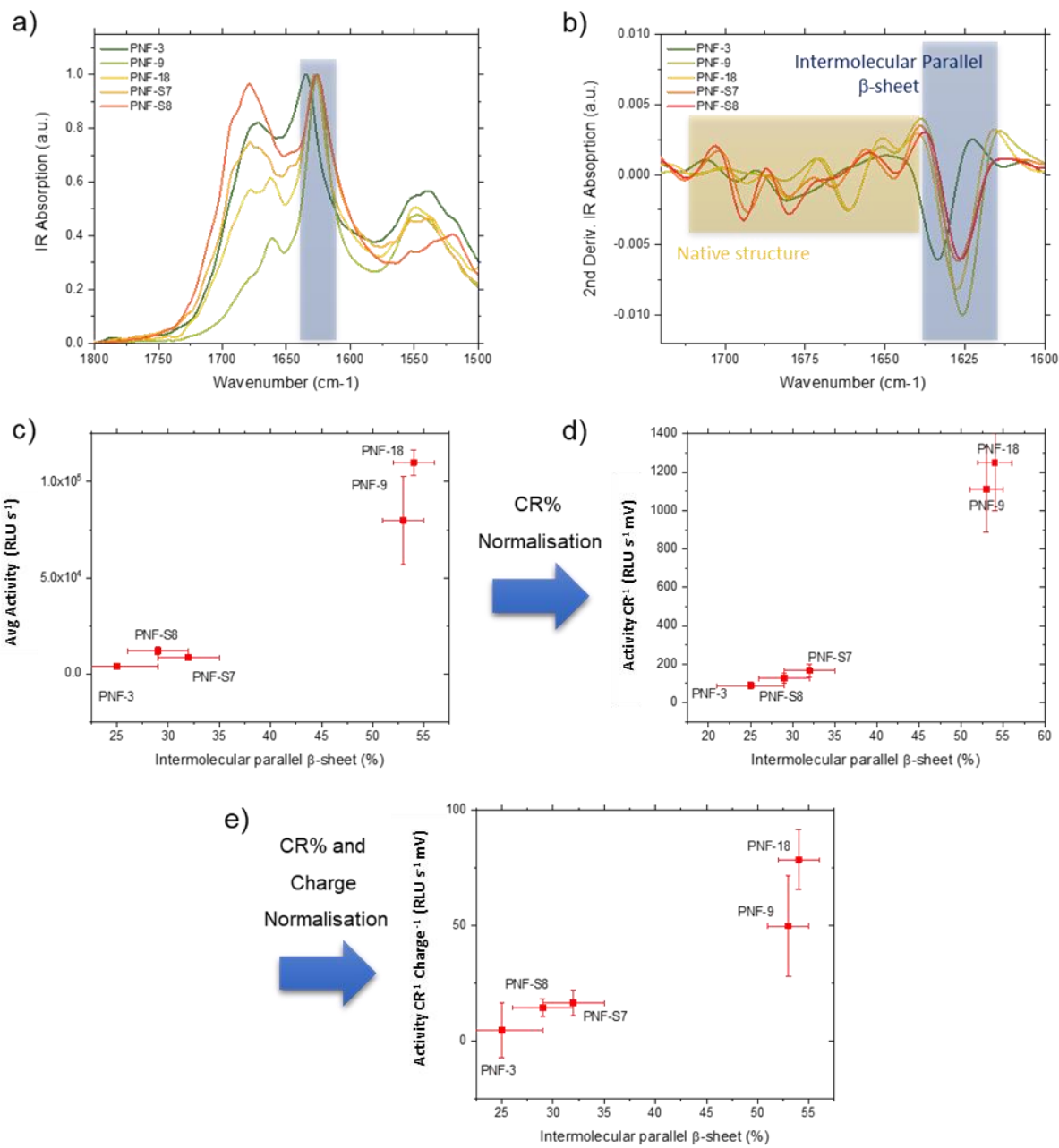


Figure S9: Structural variability upon intrinsic switch in a) presence and b) absence of the N-terminal cysteine.

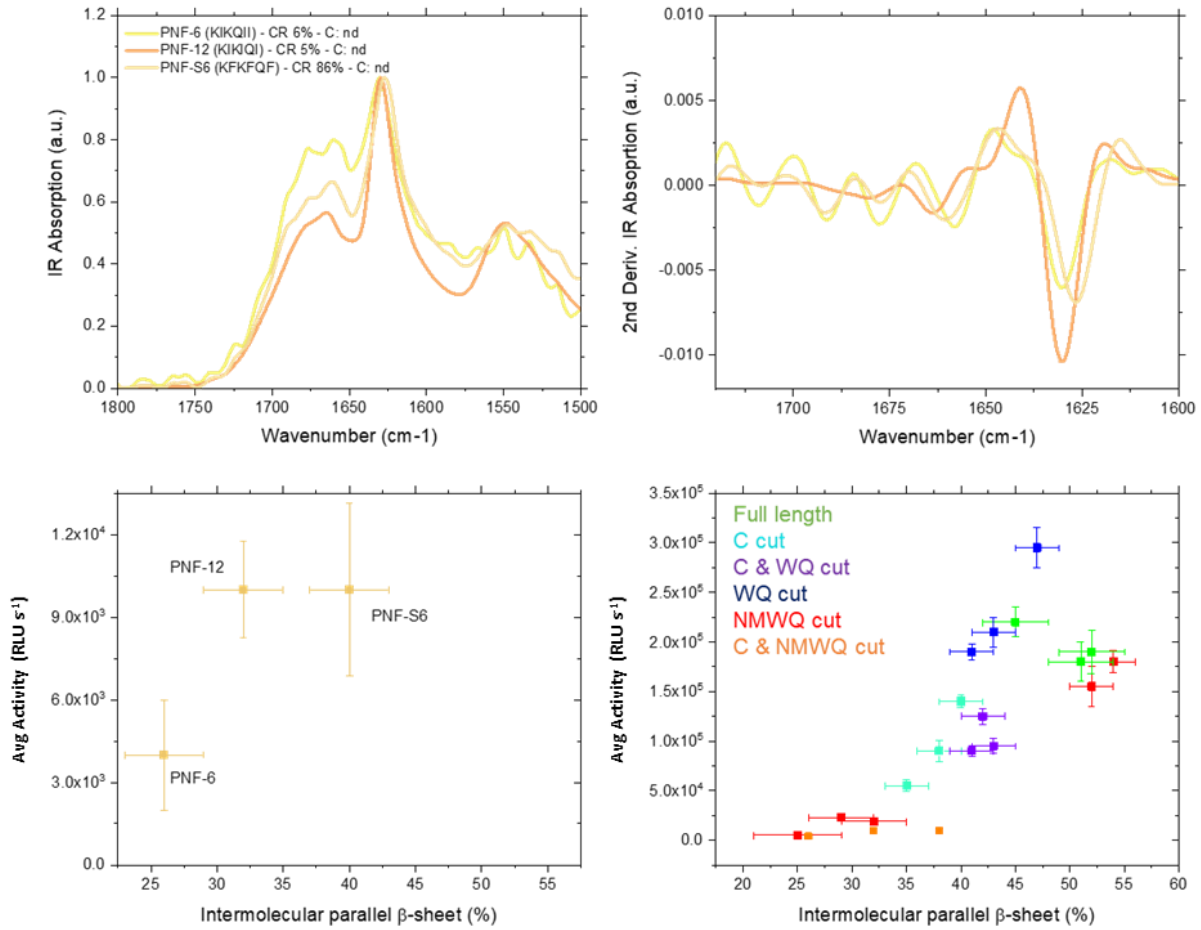


Figure S10: Structural variability vs. activity for PNF-6, -12, S6.

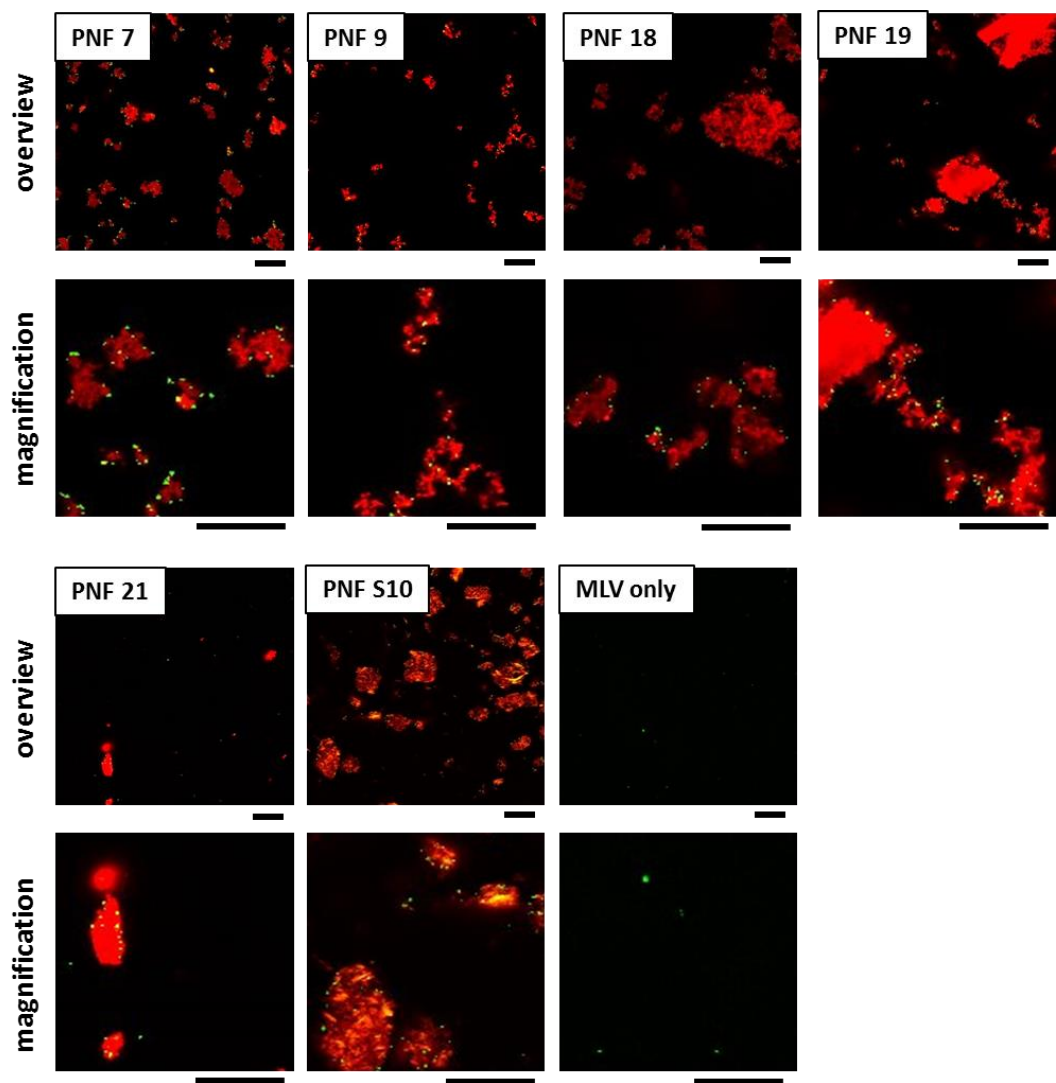


Figure S11: Laser scanning micrographs of different Proteostat® stained PNFs (red) incubated with MLV-YFP (green) to investigate attractions between fibrils and viral particles. Scale bars represent 20 μ m.

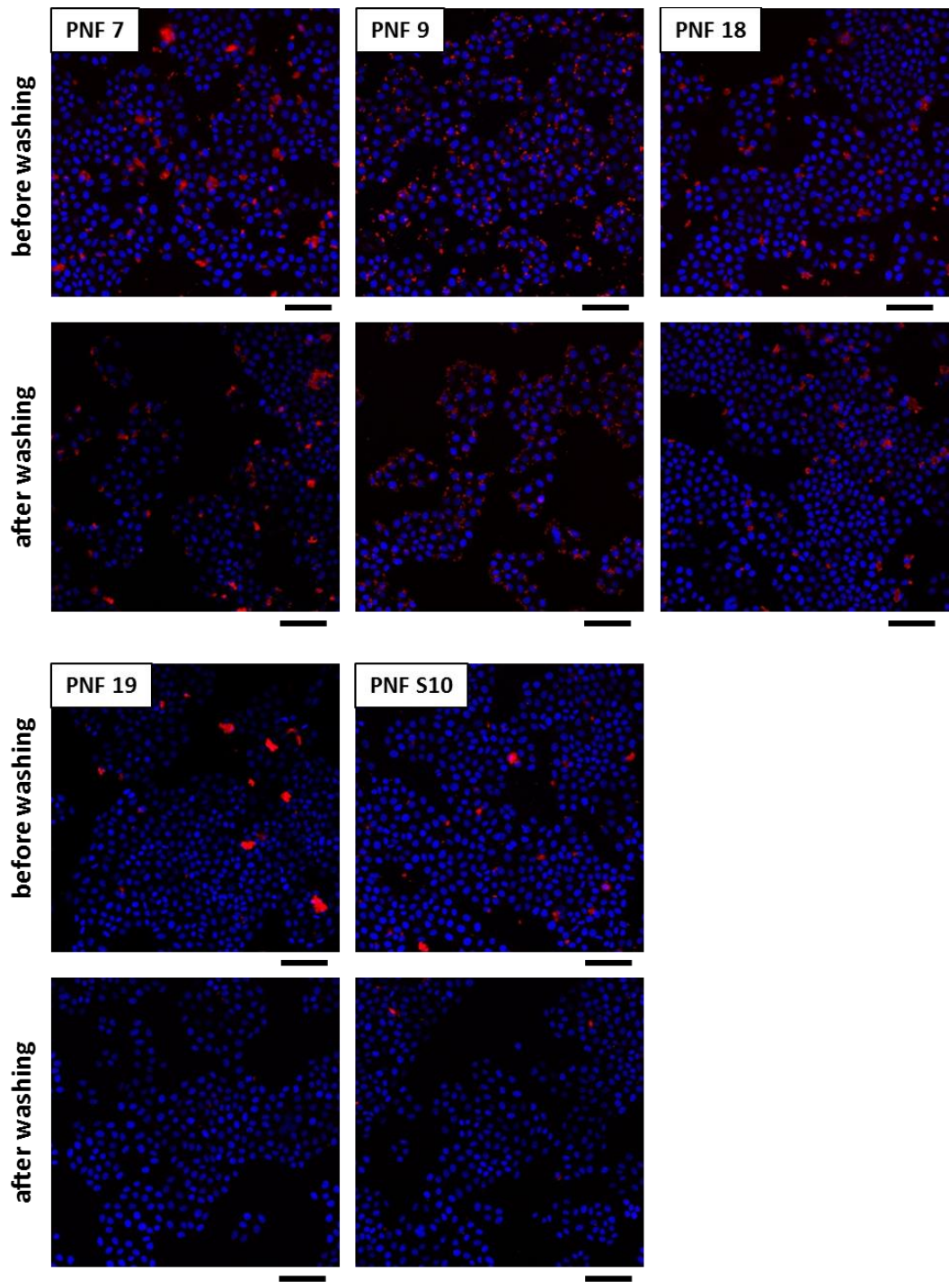


Figure S12: Laser scanning micrographs of Proteostat® stained PNFs (red) incubated on Hoechst stained TZM-bl cells (blue) for determination of PNF cell attachment before and after washing with PBS. Scale bars represent 100 μ m.

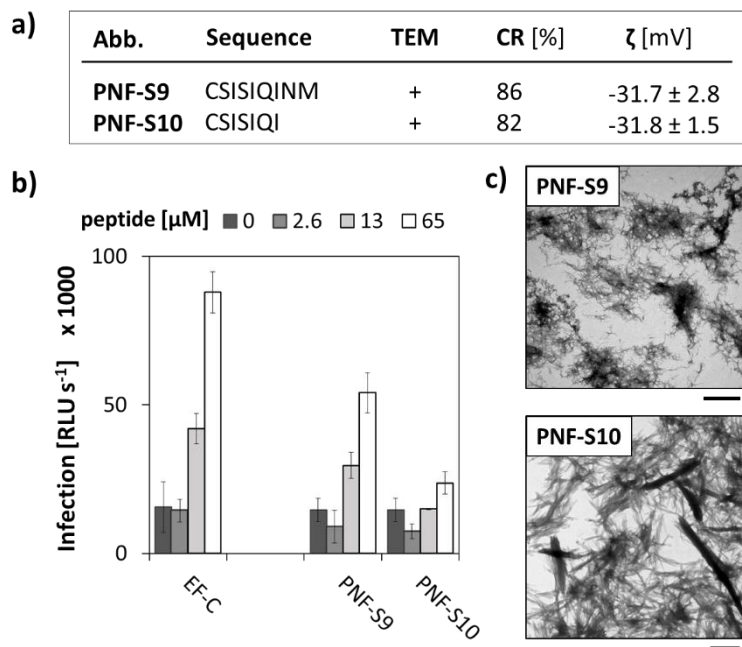
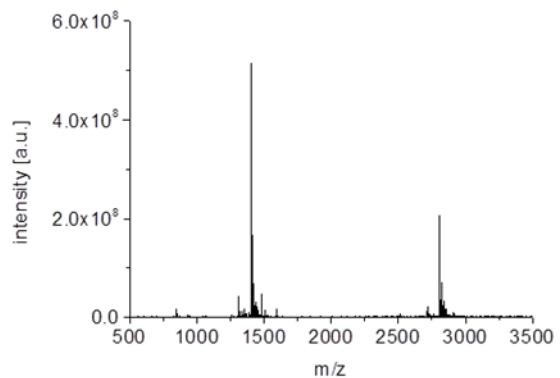
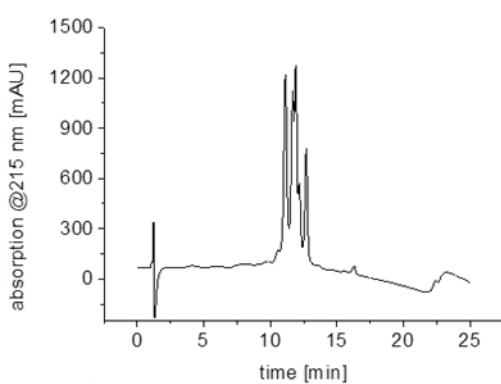
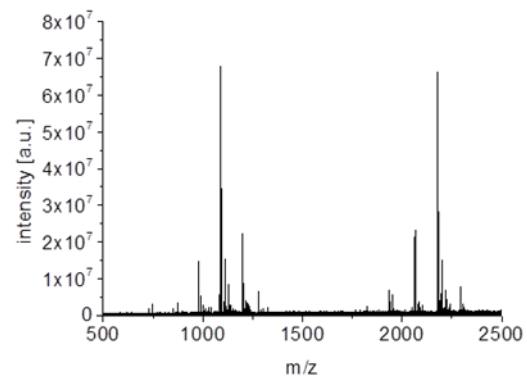
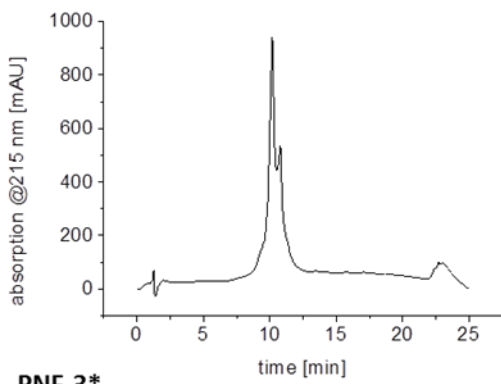


Figure S13: a) Tabular list of serine containing peptide derivatives, including the ability to form PNFs as observed in TEM measurements with + = fibrils and - = no aggregate formation detected. Monomer-to-fibril conversion rates (CR) were determined in a fluorescence-based assay. High values indicate a large percentage of peptides participating in fibril formation. Zeta potential values for PNF solutions. b) Transduction enhancement assay showing HIV-1 infection rates of TZM-bl cells observed in the presence of increasing concentrations of PNF. Shown are mean values derived from triplicate infections ± standard deviation. RLU/s; relative light units per second. c) Representative TEM micrographs of PNF assemblies. Scale bars represent 500 nm.

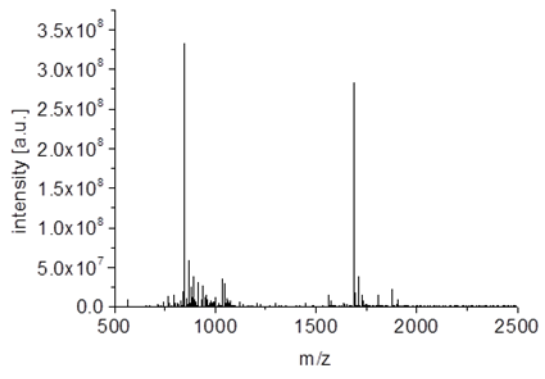
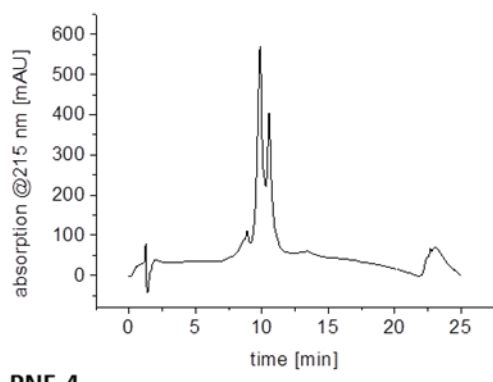
PNF-1



PNF-2*



PNF-3*



PNF-4

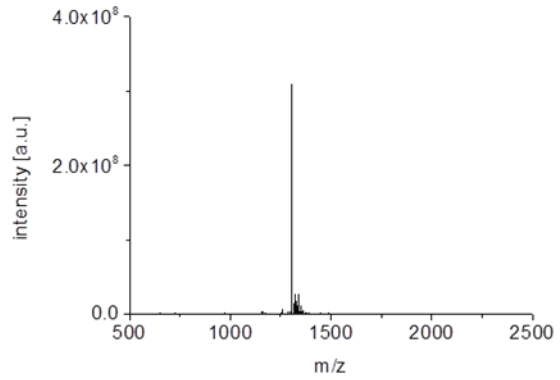
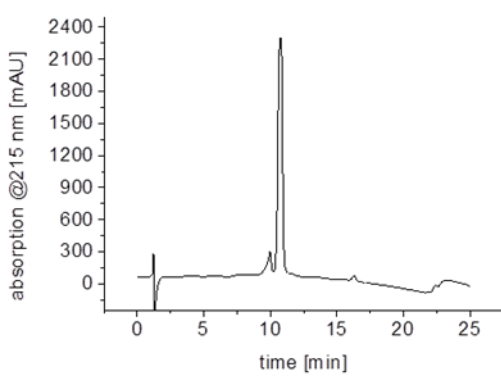
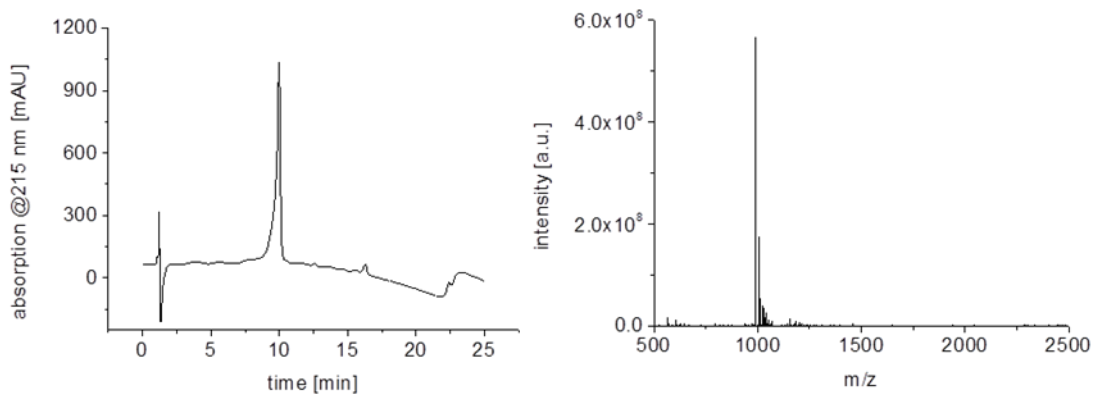
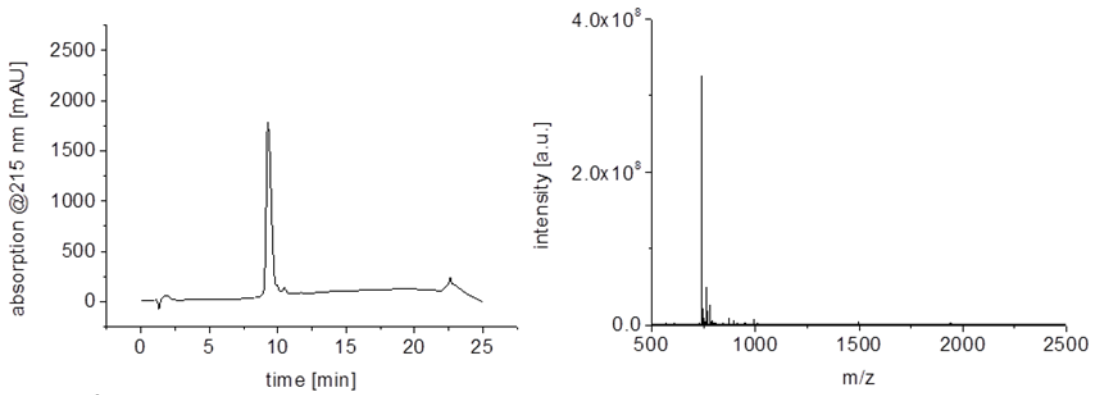


Figure S14: ctnd.

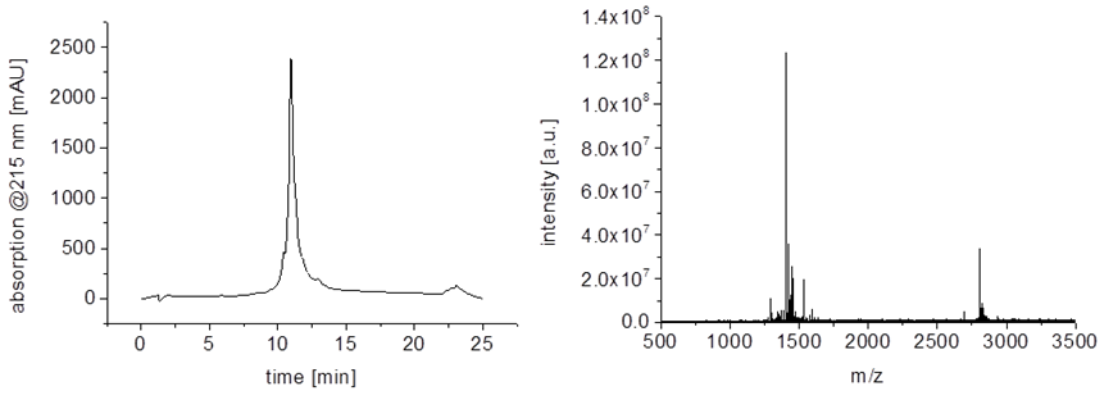
PNF-5



PNF-6



PNF-7*



PNF-8*

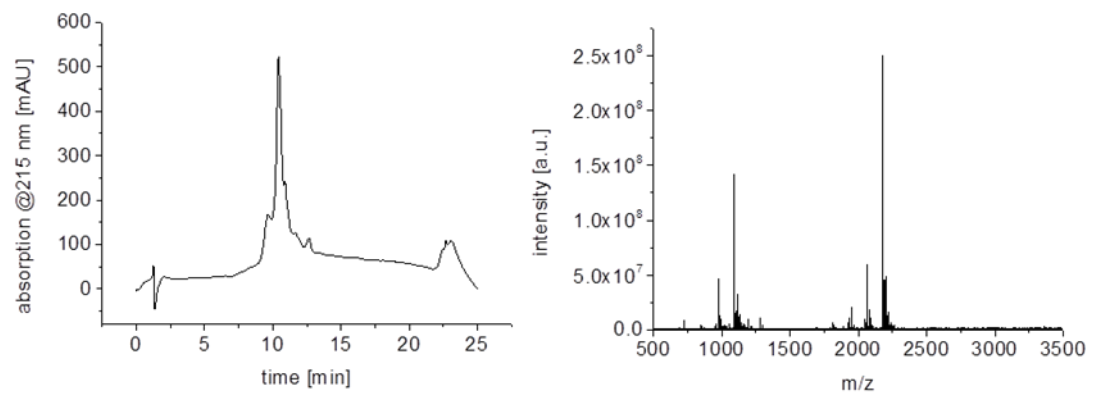
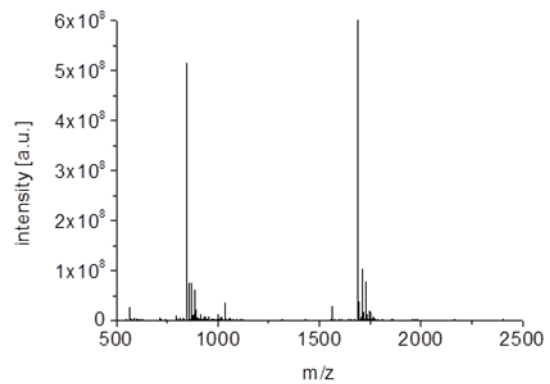
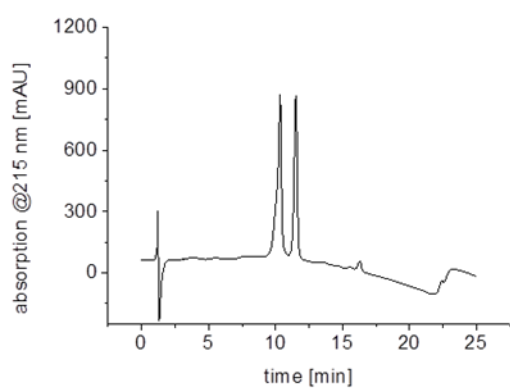
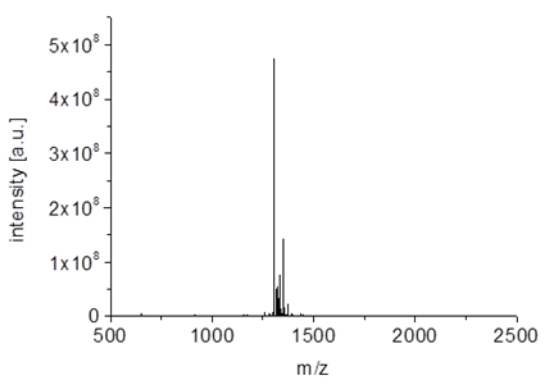
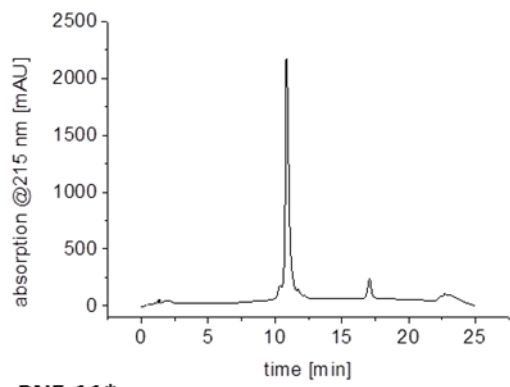


Figure S14: ctnd.

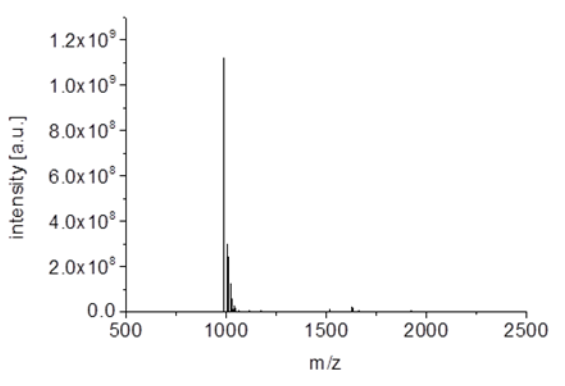
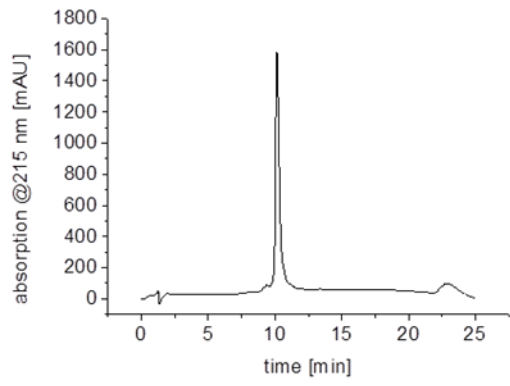
PNF-9



PNF-10*



PNF-11*



PNF-12*

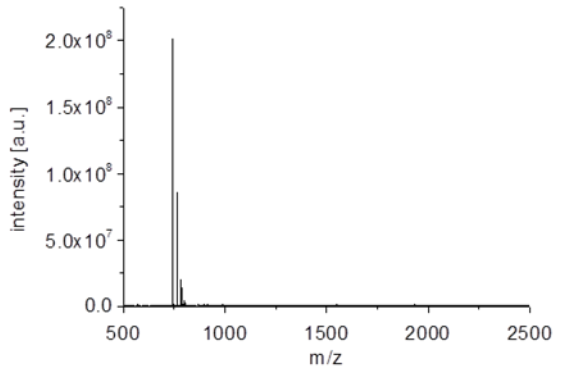
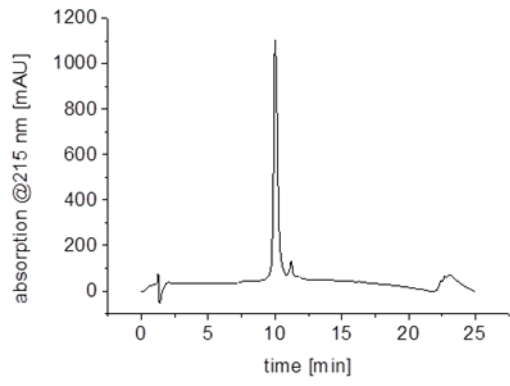
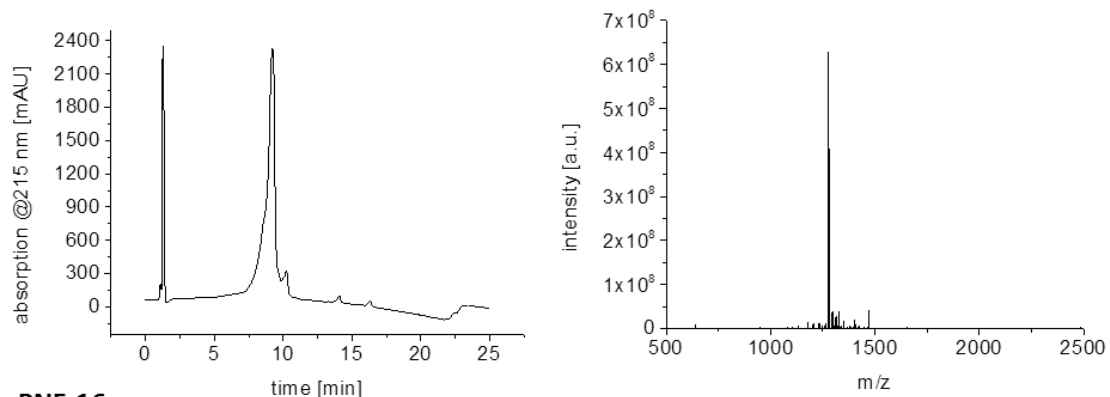
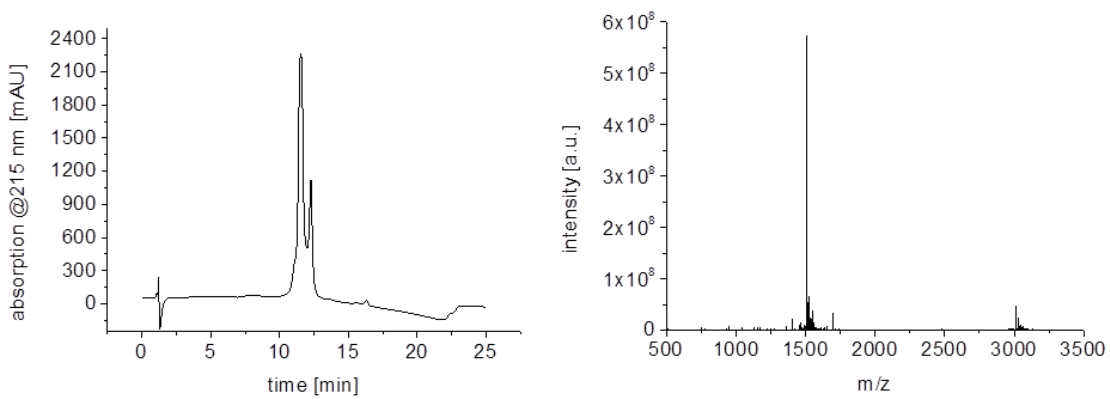


Figure S14: ctnd.

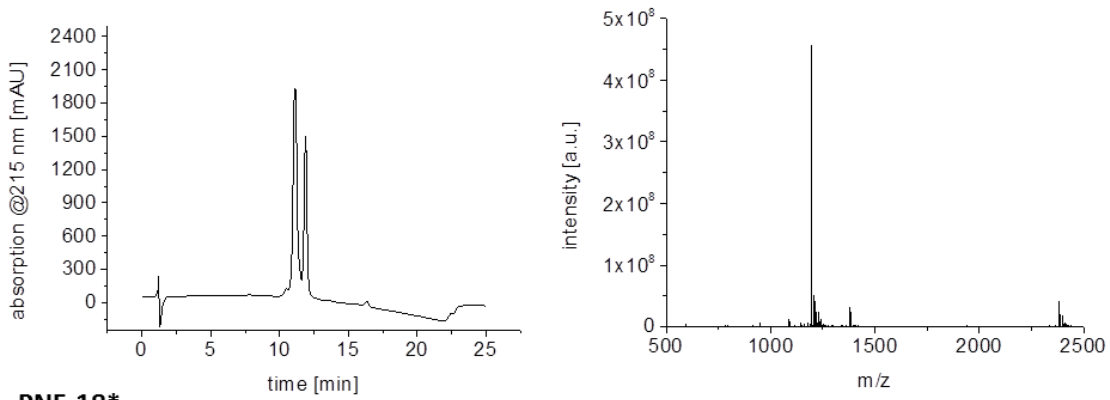
PNF-13



PNF-16



PNF-17



PNF-18*

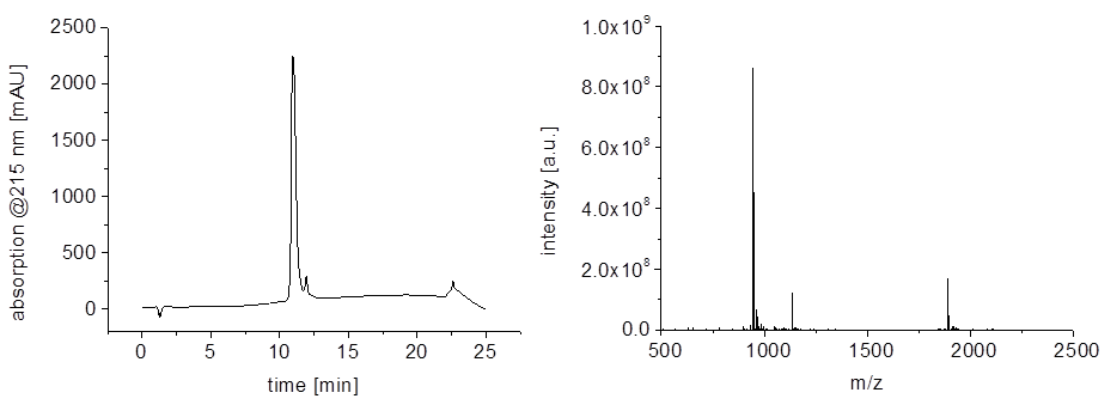
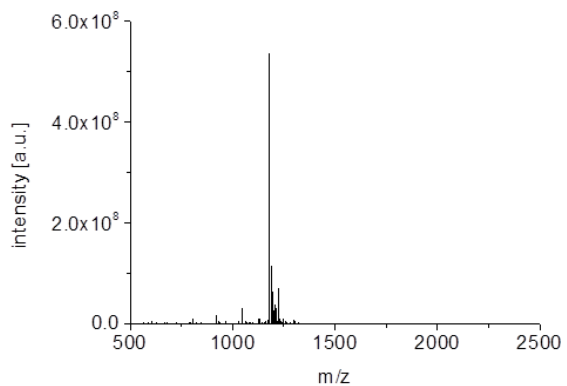
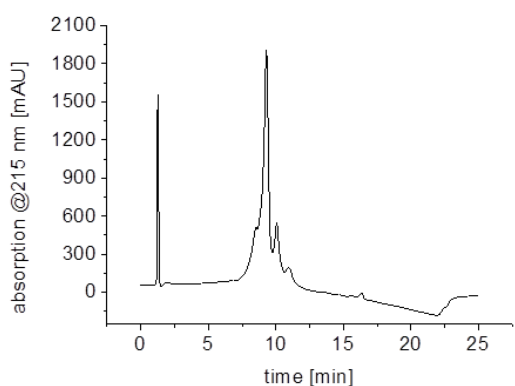
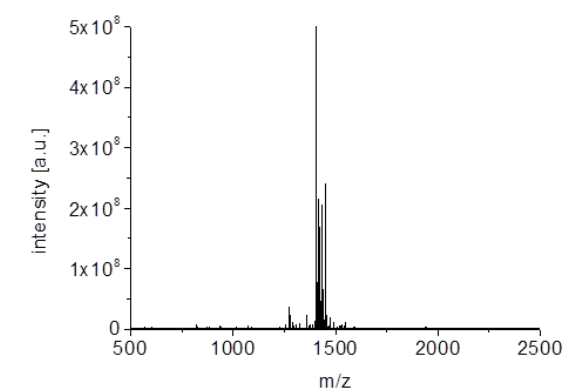
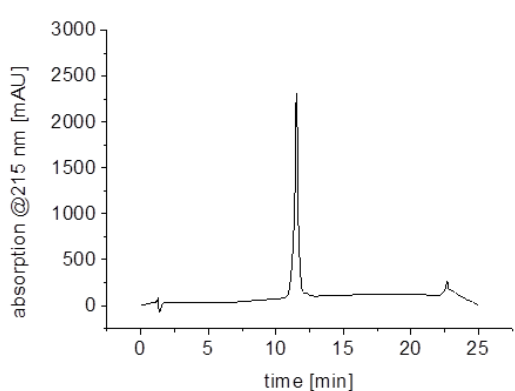


Figure S14: ctnd.

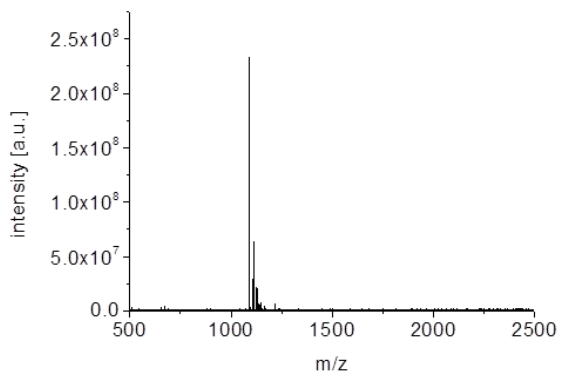
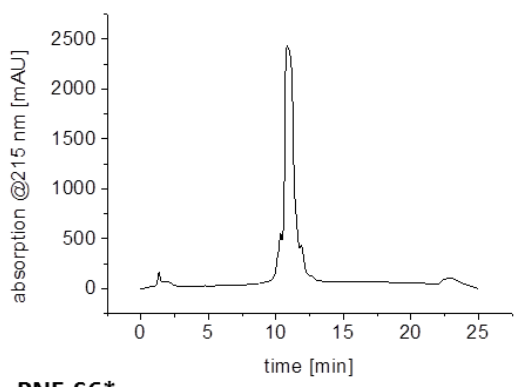
PNF-S1



PNF-S4



PNF-S5*



PNF-S6*

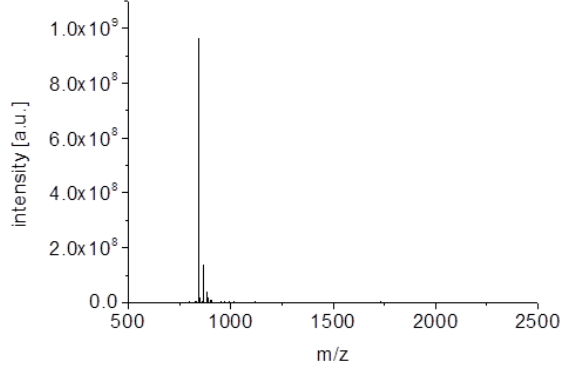
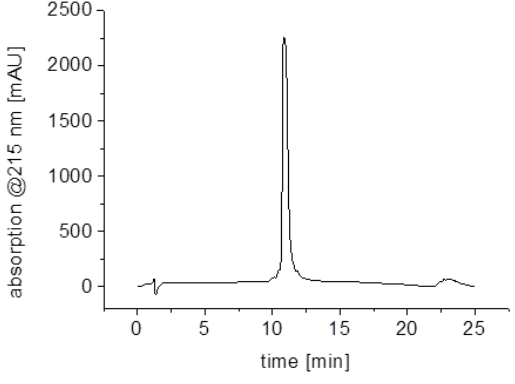
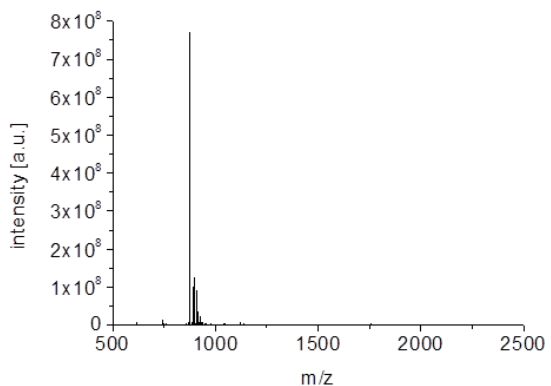
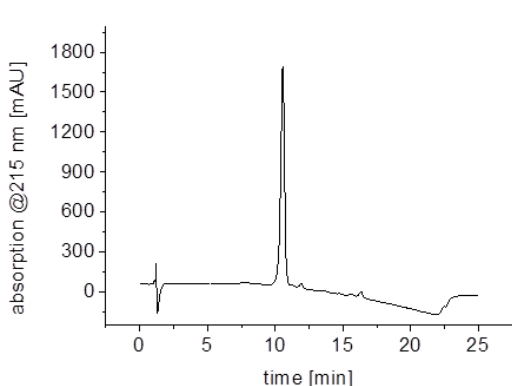


Figure S14: ctnd.

PNF-S7



PNF-S8

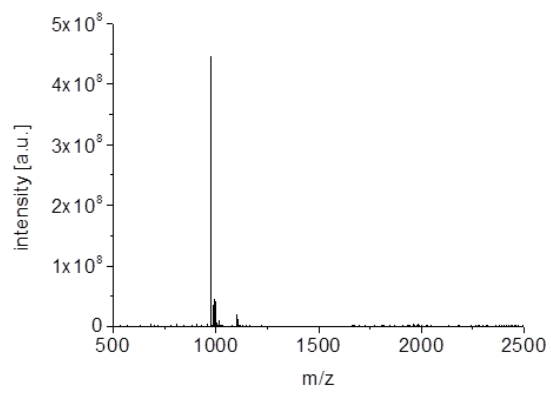
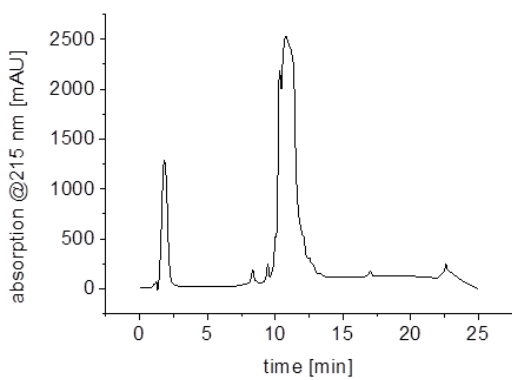


Figure S14: High performance liquid chromatograms of PNFs and corresponding MALDI spectra of purified fractions. Entries marked with * have previously been published.^[1]

References

- [1] C. Schilling, T. Mack, S. Lickfett, S. Sieste, F. S. Ruggeri, T. Sneideris, A. Dutta, T. Bereau, R. Naraghi, D. Sinske, T. P. J. Knowles, C. V. Synatschke, T. Weil, B. Knöll, *Adv. Funct. Mater.* **2019**, *29*, 1809122.
- [2] M. Yolamanova, *Ph.D. Thesis*, Univeristy Ulm, **2016**.
- [3] A. Papkalla, J. Münch, C. Otto, F. Kirchhoff, *J. Virol.* **2002**, *76*, 8455.